



Published in final edited form as:

Echocardiography. 2015 February ; 32(2): 349–360. doi:10.1111/echo.12636.

Comparison of Quantitative Wall Motion Analysis and Strain For Detection Of Coronary Stenosis With Three-Dimensional Dobutamine Stress Echocardiography

Katherine M. Parker, Ph.D.¹, Alexander P. Clark¹, Norman C. Goodman, B.S.², David K. Glover, Ph.D.^{2,3}, and Jeffrey W. Holmes, M.D., Ph.D.^{1,2,3}

¹Department of Biomedical Engineering, University of Virginia, Charlottesville, VA

²Department of Medicine, University of Virginia, Charlottesville, VA

³Department of Robert M. Berne Cardiovascular Research Center, University of Virginia, Charlottesville, VA

Abstract

Background—Quantitative analysis of wall motion from three-dimensional (3D) dobutamine stress echocardiography (DSE) could provide additional diagnostic information not available from qualitative analysis. In this study we compare the effectiveness of 3D fractional shortening (3DFS), a measure of wall motion computed from 3D echocardiography (3DE), to strain and strain rate measured with sonomicrometry for detecting critical stenoses during DSE.

Methods—Eleven open-chest dogs underwent DSE both with and without a critical stenosis. 3DFS was measured from 3DE images acquired at peak stress. 3DFS was normalized by subtracting average 3DFS during control peak stress (3DFS). Strains in the perfusion defect (PD) were measured from sonomicrometry, and PD size and location were measured with microspheres.

Results—A 3DFS abnormality indicated the presence of a critical stenosis with high sensitivity and specificity (88% and 100%, respectively), and 3DFS abnormality size correlated with PD size ($R^2=0.54$). The sensitivity and specificity for 3DFS was similar to that for area strain (88%, 100%) and circumferential strain and strain rate (88%, 92% and 88%, 86%, respectively), while longitudinal strain and strain rate were less specific. 3DFS correlated significantly with both coronary flow reserve ($R^2=0.71$) and PD size ($R^2=0.97$), while area strain correlated with PD size only ($R^2=0.67$), and other measures were not significantly correlated with flow reserve or PD size.

Conclusion—Quantitative wall motion analysis using 3DFS is effective for detecting critical stenoses during DSE, performing similarly to 3D strain, and provides potentially useful information on the size and location of a perfusion defect.

Keywords

Demand ischemia; Coronary artery disease; Cardiac mechanics; Perfusion; Three dimensional transthoracic echocardiography; Strain; Strain rate imaging; Stress echocardiography; Wall motion

INTRODUCTION

Dobutamine stress echocardiography (DSE) is one of the most commonly-used methods for diagnosing coronary artery disease (CAD). However, visual diagnosis of wall motion abnormalities during DSE suffers from relatively low interobserver agreement¹ due to the qualitative nature of diagnosis and its reliance on the expertise of the cardiologist.² The use of quantitative measures is expected to improve accuracy and objectivity of echo image analysis,³ and numerous methods for measuring regional wall motion,^{4,5} strain,^{6,7} and strain rate^{8,9} during DSE have been developed for implementation in two-dimensional (2D) echo. However, the reproducibility of quantitative measures in 2D echo has been limited by angle dependence, through-plane motion, variation between vendors, and difficulty in defining a center axis for fractional shortening measurement that is not affected by ischemic bulging.¹⁰⁻¹² Because of these issues, no quantitative measurement is currently considered ready for routine clinical use for diagnosis of CAD during DSE.³

DSE using three-dimensional (3D) echocardiography (3DE) has been shown to be diagnostically equivalent to 2D echo,¹³ and 3DE-based measures of mechanical function may overcome many of the limitations of 2D measures. Previously, our group developed a measure of wall motion from 3DE called three-dimensional fractional shortening (3DFS), and showed that 3DFS could be used to detect wall motion abnormalities in a finite element model of ischemia¹⁴ and during transient coronary occlusion in dogs.¹⁵ Other groups have developed methods for measuring myocardial strain from 3DE using speckle tracking,¹⁶ and have proposed area strain as a measure that takes advantage of the 3D data and is more sensitive to mechanical abnormalities than circumferential or longitudinal strain.^{17,18} Developing quantitative 3D measures for detecting mechanical abnormalities that indicate CAD during stress testing is one of the most challenging applications of 3DE due to the increased heart rate and small time frame for acquisition. The goal of this study was to evaluate the effectiveness of 3DFS for detecting critical stenoses during DSE, and to compare 3DFS to strain and strain rate in the ischemic region measured by sonomicrometry, a gold-standard measure of myocardial deformation.

METHODS

Surgical Preparation

This experimental protocol was approved by the Institutional Animal Care and use Committee at the University of Virginia. Eleven adult mongrel dogs (body weight 21.7 ± 1.5 kg) were anesthetized with 0.5mg fentanyl citrate and 40mg etomidate and maintained using 1.5-2.5% isoflurane gas. A left thoracotomy was performed and instrumentation was placed using methods described previously.^{15,19} A Millar pressure catheter (Mikro-Tip SPC-454D, Millar Instruments, Houston, TX) was inserted into the left ventricle (LV) to

measure pressure (LVP). The left anterior descending (LAD) coronary artery was isolated, a snare ligature was loosely placed proximal to the first diagonal, and instrumentation was placed as illustrated in Figure 1A. An ultrasonic flow probe (model T-206, Transonic Systems, Ithaca, NY) was placed distal to the snare and the space between the probe and vessel wall was filled with an acoustic gel. Nine sonomicrometer crystals (2T-36S-40-RS, Sonometrics, London, Ontario, Canada) were inserted into the LV midwall: six to measure changes in length of the three axes of the LV (anterior-posterior, septal-lateral, and base-apex), while the remaining three crystals were placed in the anterior LV wall at a depth of 7-10mm, in the region supplied by the LAD, to measure midwall strains in the circumferential-longitudinal plane. During each data acquisition, ECG, arterial pressure, LAD flow, LVP, and sonomicrometry signals were recorded at a frequency of 195 Hz.

Experimental Protocol

A standard dobutamine stress protocol was performed on each animal both without (CTRL) and with (STEN) a critical stenosis in the LAD artery, as diagrammed in Figure 1B. After surgery and instrumentation, dobutamine was infused in 5-minute dose increments of 5, 10, 20 and 30 μ g/kg/min. Data acquisition was performed at baseline and at the end of the 30 μ g/kg/min dobutamine dose, including apical 3DE images acquired using a Sonos 7500 ultrasound system (Philips Medical Systems, Andover, MA). A silicone gel standoff (Aquaflex, Parker Laboratories, Fairfield, NJ) was placed between the x4 ultrasound probe and the apex of the heart, and full volume images were acquired over four beats. Radiolabeled microspheres (diameter 15 μ m labeled with Sr-85, Nb-95, or Sc-46, Perkin-Elmer, Boston, MA) were injected into the left atrial catheter at baseline and at each maximum dobutamine dose. After the maximum dobutamine dose, dobutamine infusion was stopped and cardiac function gradually returned to baseline. After 45 minutes, data acquisition was performed and a critical LAD stenosis was set as described previously.¹⁹ The LAD snare ligature was tightened as much as possible without reducing flow, and the hyperemic response was measured by occluding the LAD for 10 seconds and observing the peak hyperemic flow that followed. The snare ligature was then adjusted so that the reactive hyperemic response was abolished. After setting the stenosis, the dobutamine stress protocol, data acquisition, and microsphere injection were repeated. The animals were euthanized with a lethal dose of pentobarbital and hearts were excised for imaging of sonomicrometer placement and microsphere analysis.

Assessment of Functional Data and Regional Strain

Hemodynamic data were processed using the Sonometrics software, SonoSoft®, and custom Matlab software (Mathworks, Natick, MA). LV volume, heart rate, and regional strains were calculated using methods described previously.^{20,21} Coronary flow reserve (CFR) was calculated by dividing the LAD flow measured by the flow probe during peak stress by flow measured just before dobutamine administration. As some animals still exhibited substantial increases in coronary flow with dobutamine infusion during STEN, only stenoses with CFR<1.1 during stress were considered critical stenoses. Measures were evaluated on their ability to separate these critical stenoses from CTRL and STEN with CFR>1.1.

Area strain, or the fractional change in the area of the sonomicrometer triangle ($(A_{ES}-A_{ED})/A_{ED}$), was computed as the product of principal strains minus 1. Strain rate in the circumferential and longitudinal directions was measured by taking the derivative of strain with respect to time. Temporal averaging of the strain rate curves was used with a window of 10ms. Peak systolic strain rate was calculated as the peak negative strain observed between the opening of the aortic valve, defined by the time after ED when LV volume begins changing, and closing of the aortic valve, or ES. This is the same strain rate parameter most often used with Doppler echocardiography to detect strain rate abnormalities.²²⁻²⁴

Assessment of Regional Myocardial Blood Flow

After the experiment, the heart was fixed in formalin and sectioned into 60 transmural blocks evenly distributed over the LV surface as illustrated previously.¹⁵ Regional myocardial blood flow was determined for each block using standard methods for quantification of radioactive microspheres.¹⁹ Myocardial flow reserve (MFR) was determined for each block by dividing the flow during peak stress by baseline flow from the first microsphere injection. Size of the perfusion defect (PD) was defined as the fraction of blocks in which the MFR was less than 1.1, the same as the CFR cutoff for a critical stenosis.

Quantitative Wall Motion Analysis

The 3DE images were exported to CD and segmented using Tomtec 4D LV-Analysis® software version 2.6 (Tomtec Imaging Systems, Unterschleissheim, Germany). The software generated a surface representing the LV endocardial border at ED and ES from three initial contours, and the user manually edited the surface as necessary (Figure 2A). A cloud of points representing the final endocardial surface was exported in Cartesian coordinates and analyzed using custom software written in Matlab as described previously.^{14,15} The endocardial data were transformed into a cardiac coordinate system using three anatomical landmarks selected at ED: the apex, base, and middle of the septum. This cardiac coordinate system has axes directed parallel to the base-apex axis (x_1), through the mid-septum (x_2), and through the posterior wall (x_3) from an origin located 1/3 of the distance from the base to apex along the LV long axis.

Parametric surfaces were fit through the data in prolate spheroidal coordinates, illustrated in Figure 2B. In this elliptical coordinate system, every point on the LV surface is represented by circumferential (θ) and longitudinal (μ) angles from the origin and a radial distance along an arc from the central axis $\lambda=\lambda(\mu,\theta)$ (Figure 2C). Fitting was performed, as described previously,¹⁴ using a mesh with 4 circumferential and 4 longitudinal elements. 3DFS was calculated as the fractional change in λ between ED and ES ($3DFS = (\lambda_{ED} - \lambda_{ES}) / \lambda_{ED}$) at each location on the surface. The 3DFS during CTRL peak stress averaged across all dogs for each location is displayed on a Hammer projection map (top) and a standard bulls-eye map (bottom) in Figure 2D. The Hammer projection preserves relative surface areas, so that the size of any region of interest on the map reflects its true size as a fraction of LV surface area; by contrast, on a bulls-eye map the basal segments appear larger than their true size, while the apical segments appear smaller. For this reason, Hammer maps are used for

visualization in this report. On average, 3DFS steadily increases from the base to the apex; any measure of abnormal wall motion must therefore detect differences from this pattern. To account for this inhomogeneity, three different methods of normalizing regional 3DFS to compute 3DFS were evaluated: 1) subtract the average peak stress 3DFS during CTRL at each location, 2) subtract the average resting 3DFS during CTRL at each location, and 3) subtract individual resting 3DFS for that subject at each location. These three options were chosen because they are clinically available. Average resting or peak stress 3DFS may be measured in volunteers without CAD, and baseline images can be acquired for each individual before dobutamine infusion. Each measure was evaluated for sensitivity and specificity of separating $CFR < 1.1$ from $CFR > 1.1$, where the presence of an abnormal 3DFS region larger than 5% of the LV surface in an experiment with a critical stenosis ($CFR < 1.1$) was defined as a positive test. These ROC curves are displayed in Figure 3. Normalization by average stress CTRL 3DFS was the most sensitive and specific for detecting a critical stenosis, so 3DFS was defined as 3DFS during peak stress for each experiment minus 3DFS during CTRL peak stress averaged for all dogs. The size of a 3DFS abnormality was computed as the fraction of the surface area of the LV with 3DFS below a threshold determined using ROC analysis, where the presence of an abnormal 3DFS region larger than 5% of the LV surface in an experiment with a critical stenosis ($CFR < 1.1$) was a true positive test. For comparisons with strain, 3DFS in the center of the PD was measured by averaging 3DFS in the locations of the tissue blocks containing the sonomicrometer crystals.

Statistical Analysis

All values are reported as mean \pm SD. Changes in hemodynamic variables between CTRL and STEN were assessed using a paired t-test. Linear regression was performed using Microsoft Excel 2007 Data Analysis ToolPak, and overall significance of the regression was calculated using the F-test statistic. Receiver operating characteristic (ROC) curves²⁵ were used to compare the diagnostic utility of different measures of regional mechanics by measuring the optimal sensitivity and specificity and the area under the curve (AUC) for separating experiments in which $CFR < 1.1$ from $CFR > 1.1$. Significance of ROC curves for detecting $CFR > 1.1$ was calculated with unpaired analysis in GraphPad Prism software (GraphPad Software, San Diego, CA).

RESULTS

A total of 22 dobutamine stress tests were performed, with one CTRL and one STEN in each dog. One CTRL experiment was excluded because the 3DE image quality during peak stress was poor. Hemodynamic data acquired at baseline and peak stress for CTRL and STEN are summarized in Table 1. Heart rates and volumes were very similar during peak stress for CTRL and STEN, while systolic pressure and LAD flow were smaller during STEN as expected. Average CFR in the LAD was 1.08 ± 0.49 during STEN compared with 3.23 ± 1.61 during CTRL, and average PD size during STEN was $26 \pm 15\%$ of LV mass, ranging from 2 to 47%. Of the 11 STEN experiments, 8 had $CFR < 1.1$ and 3 displayed greater increases in flow. In the $CFR < 1.1$ experiments, average CFR was 0.86 ± 0.15 and average PD size was $31 \pm 13\%$, ranging from 15 to 47%.

Detecting Critical Stenoses

Wall Motion Analysis—A Hammer map of the average 3DFS during CTRL peak stress is shown in Figure 2D, where each location on the LV surface represents the average 3DFS in that location over 10 dogs. The mean standard deviation in 3DFS over all locations was 0.12. 3DFS maps were produced for each STEN image at peak stress. The optimal threshold determined by ROC analysis for detecting regions of abnormal 3DFS in experiments with $CFR < 1.1$ and not in those with $CFR > 1.1$, including CTRL and three STEN experiments, was $3DFS < -0.275$. With this threshold, the presence of an abnormal 3DFS region indicated the presence of a critical stenosis with 88% sensitivity and 100% specificity (Table 2). As 3DFS was measured over the entire LV surface, the size and location of a region with decreased wall motion should provide information on the size and location of the PD. An example comparing the PD and abnormal 3DFS regions in a typical dog is shown in Figure 4A. The abnormal 3DFS region is smaller but contained within the PD. Across all STEN experiments, 97% of locations within the abnormal 3DFS region were also contained in the PD. In STEN cases with $CFR < 1.1$, the size of the abnormal 3DFS region correlated well with the PD size (Figure 4B).

Comparison of Wall Motion and Strain—The efficacy of detecting a critical stenosis with 3DFS was compared to area, circumferential, and longitudinal strain and peak systolic strain rates measured by sonomicrometry. ROC analysis was used to determine the sensitivity and specificity of each measure for separating $CFR < 1.1$ from $CFR > 1.1$. Figure 5 shows ROC curves for all six measures. All curves were significant ($p < 0.05$) for detecting $CFR < 1.1$. 3DFS, area strain, and circumferential strain and strain rate showed similar sensitivity, specificity, and AUC, while longitudinal strain and strain rate appeared to be less specific (Figure 5, Table 2).

Flow-Function Behavior

Because both the size of an ischemic region and the severity of the flow restriction induced by stress could affect regional mechanics, linear regression was used to test the individual effects of PD size and CFR on 3DFS and strain measured in the center of the PD region during STEN. All cases with $CFR < 2.0$ were included in the fits, including those where the stenosis was not critical, to evaluate each measure in cases with CFR near the critical stenosis definition. Fit quality, slopes, and significance are displayed in Table 3. PD size was expressed as a fraction of LV mass for regression. CFR ranged from 0.75 to 2.42, and PD size from 0.02 to 0.47. 3DFS regressions were significant both with CFR and with PD size as the predictor variable. Surprisingly, area strain regressions were only significant with PD size as the predictor variable, not CFR. Regressions of circumferential and longitudinal strain and strain rate with were not significant with CFR or PD size. Figure 6 shows more detail of this flow-function behavior. Area strain displays the expected exponential flow-function behavior when both STEN and CTRL are plotted together (Figure 6A). When focusing only on the cases where $CFR < 2.0$ and regressions were significant (Figure 6B-D), area strain became more positive (less shortening) with increasing PD size, while 3DFS became more negative (less inward motion or more outward bulging) with increasing PD size and decreasing CFR.

DISCUSSION

In this study we evaluated the effectiveness of 3DFS for diagnosing critical stenoses during cardiac stress testing, and compared the results to strain measured by sonomicrometry. Our results show that 3DFS can be used to detect a critical stenosis with excellent sensitivity and specificity as well as to measure the size and location of a PD, and is influenced by both CFR and PD size. In comparison, area strain displayed similar diagnostic utility to 3DFS while longitudinal strain and strain rate did not perform as well. One surprising finding, as mechanical function has traditionally been considered a function of blood flow, is that PD region size accounted for more of the variation in these measures of mechanical function than CFR.

Wall Motion Analysis

3DFS showed promise in this study for detecting CAD and quantifying the size of the PD during stress testing. The presence of a 3DFS abnormality indicated a critical stenosis with 88% sensitivity and 100% specificity. In comparison, the standard clinical 2D stress echocardiogram has been shown to detect angiographically-significant CAD with 80% sensitivity and 86% specificity.²⁶ Measuring function over the entire LV surface also allows quantification of the size, location, and magnitude of a mechanical abnormality. One of our original goals in developing the 3DFS measure was to quantify the size and location of an ischemic region, and we previously demonstrated close correlation between the size of an ischemic region and the size of a wall motion abnormality in both finite element modeling¹⁴ and during experimental coronary occlusion.¹⁵ In the present study, we found that the size of a 3DFS abnormality also correlates well with PD size during stress testing, and that regions identified as abnormal by 3DFS are almost always within the PD.

However, these regions of abnormal wall motion were always smaller than the perfusion abnormality. Perfusion abnormalities are known to precede mechanical abnormalities at lower doses of dobutamine and have been measured to be larger than mechanical abnormalities during stress testing.²⁷ Therefore, the observed difference between functional abnormality size and perfusion abnormality size is to be expected. This is in contrast to supply ischemia or infarcts imaged at rest, where the mechanical abnormality is generally larger than the perfusion abnormality.^{28,29} Our prior modeling and experimental studies of supply ischemia^{14,15} suggested that tethering to adjacent healthy myocardium may limit detection of small ischemic regions by wall motion-based approaches. The two smallest ischemic regions with $CFR < 1.1$ in this study were 15% of LV mass, and our analysis detected one of the two, along with all larger ischemic regions. Based on these results, we cannot yet reach any definitive conclusions about the performance of 3DFS for detection of demand ischemia affecting $< 15\%$ of LV mass. Overall, our results suggest 3DFS has excellent potential not only for identifying the presence of a critical stenosis during stress testing but also for increasing the amount of diagnostic information obtained from a stress test by taking advantage of the additional data collected in a full volume 3D echocardiogram.

Strain Analysis

Area strain measured in the center of the PD correlated well with PD size and could detect critical stenoses better than circumferential or longitudinal strain. This was expected, as area strain describes deformation in both the circumferential and longitudinal directions and previous studies showed area strain to be more sensitive to changing mechanics than circumferential or longitudinal strain.¹⁷ In comparison, even using sonomicrometry, a gold standard technique with low noise and error, circumferential and longitudinal strain correlated poorly with CFR and PD size. Previous studies have shown conflicting results in comparing circumferential and longitudinal strain for diagnosis of dobutamine-induced ischemia; some studies show circumferential strain to be superior to longitudinal,³⁰ while others claim they are diagnostically equivalent.^{31,32} Longitudinal strain was often used in the past because it was easier to measure with tissue Doppler imaging than circumferential strain. A detailed study of strains measured with radiopaque beads in dogs during brief coronary occlusion at rest showed that the amount of endocardial and midwall dyskinesis after 5 minutes of ischemia is similar in the longitudinal and circumferential directions, and the change in endocardial strain from control to ischemia was 0.19 ± 0.08 in the circumferential direction and 0.16 ± 0.06 in the longitudinal direction.³³ Therefore, some of the disagreement in the literature may be due to differences in ability to measure these two strain components with various techniques, rather than to inherent differences in mechanics in the circumferential and longitudinal directions. This further emphasizes the advantage of using area strain, which captures changes in both circumferential and longitudinal strain, when available.

Strain rate measured by tissue Doppler imaging is another commonly-used quantitative measure of regional mechanics,³⁴ and has been evaluated for detecting critical stenoses during stress testing.^{9,32,35} Longitudinal strain rate is most often reported because it is the easiest parameter to measure with tissue Doppler. However, in this study we found that peak systolic circumferential strain rate was more specific for detecting $\text{CFR} < 1.1$ than longitudinal strain rate. In fact, Figure 5 shows that the ROC curves for circumferential strain and strain rate are very similar, as are longitudinal strain and strain rate. In addition, circumferential peak systolic strain rate showed less variation during CTRL peak stress than the longitudinal direction. These results indicate that while peak systolic strain rate does not exhibit better sensitivity or specificity than strain for detecting critical stenoses, if strain rate is used then measuring in the circumferential direction is more effective for detecting critical stenoses during stress testing than the longitudinal direction.

Flow-Function Relationships

Traditionally, regional mechanical dysfunction during ischemia has been described as a function of the change in blood flow from baseline during both supply^{36,37} and demand³⁸ ischemia. However, in this study we found that strain in the center of the ischemic region correlates better with PD size than CFR during STEN. We therefore checked for potential artifacts that could contribute to this unexpected result. For example, if the sonomicrometers were not located exactly in the center of the PD region, blood flow and mechanical function could have been better near the sonomicrometers in animals with smaller PDs. We therefore plotted MFR in the tissue blocks containing the sonomicrometers against PD size to see if

MFR would decrease as PD size increases. However, MFR in this region showed no relationship with PD size ($R^2=0.042$). We also tested the sensitivity of our conclusions to the specific choice of MFR cutoff used to separate normally and abnormally perfused regions when defining PD size. Average PD size increased or decreased with the changing threshold, but the quality of correlation between PD size and AAF did not change. We conclude that during dobutamine stress, PD size is an important determinant of mechanical behavior at the center of an ischemic region and may be even more important than severity of blood flow restriction.

Application to Clinical Diagnosis

Testing 3DFS in an animal study allows us to compare our results to gold-standard measurements of perfusion and strain; the next step is to test these results clinically. 3DFS can be measured clinically with the same methods used in this study. In visual wall motion analysis, the primary source of error is the subjective nature of the assessment, which leads to substantial interobserver variability. In a study of clinical interpretation of 2D stress echocardiography, four of the five centers agreed in only 73% of patients.¹ Using 3D non-contrast stress echo, Nemes et al. found that two observers agreed on the presence or absence of ischemia in just 79% of the coronary territories.³⁹ In our quantitative wall motion analysis, the primary source of error is segmentation of the endocardial surface. Mor-Avi et al. have shown that the standard deviation of volumes computed from segmentation of RT3D images by different observers is 8% of the mean end-diastolic volume (EDV) and 13% of the mean end-systolic volume (ESV).⁴⁰ Using data from our previously published study of supply ischemia in a canine model,¹⁵ we similarly found relative standard deviations across 5 observers of 9% for EDV and 12% for ESV.⁴¹ Regional wall motion analysis is more susceptible to small, local segmentation errors that tend to cancel out in volume calculations. Therefore, we found a somewhat higher variability of abnormal area fractions (AAFs) computed from the same segmentations: the standard deviation of AAF across the 5 observers was 6% of the endocardial surface for a group of occlusions with an average size of 25%. However, the average error in AAF compared to ischemic region sized assessed by microspheres ranged from $2\pm 12\%$ to $8\pm 13\%$ for the 5 observers, compared to 14% and 19% for visual assessment of the number of segments affected.^{15,41} These results suggest that user-assisted segmentation using current commercial software is sufficient to yield consistent, accurate estimates of ischemic region size from 3DFS. In addition, semi-automatic segmentation software for 3DE continues to improve in both accuracy and ease of use, reducing the time required for clinical application of 3DFS.^{42,43}

Error in measuring strain, on the other hand, is much higher when measured clinically with speckle tracking than in the sonomicrometry data used in this study. Further, the accuracy of 3D speckle tracking measurement is highly dependent on frame rate,⁴⁴ and therefore speckle tracking during peak stress is more prone to error than at rest. To get a rough idea of how strain measured from speckle tracking would compare to 3DFS in this study, we performed a Monte Carlo simulation of expected speckle tracking strains based on our sonomicrometry measurements. We used the Bland-Altman bias and standard deviation values available in literature for comparisons of circumferential and longitudinal strain derived from 2D⁶ and 3D¹⁶ speckle tracking and area strain derived from 3D speckle tracking¹⁷ vs.

sonomicrometry to generate a probability distribution of expected speckle tracking measurements for each sonomicrometry measurement performed in our study. Table 4 details the average ROC analysis results from 1000 simulations. Due to higher error in 3D speckle tracking, we find that circumferential strain measured from 2D echo has the highest predicted AUC for detecting $CFR > 1.1$ in this analysis, followed closely by area strain. With the addition of this estimated error, AUC for area strain and circumferential strain are not different than that for 3DFS in this study, while longitudinal strain still performs less well. This reinforces our observation that 3DFS, area strain, and circumferential strain all appear to perform similarly for diagnosing critical stenoses during DSE.

Sources of Error, Limitations, and Future Directions

The primary source of error in 3DFS measurement is the variation in manual endocardial segmentation, discussed above. Another potential source of error in the present study is the lingering effect of the first stress test on the second stress test in each animal. However, we found that the difference in function between the first baseline and the second was negligible. The mean difference between the average 3DFS at each location on the LV surface at the first baseline and the second was 0.002, and LAD flow was not significantly different between baselines. Heart rate and LV volumes and pressures at ED were not significantly different ($p < 0.05$), while LV pressure was only slightly depressed and LV volume slightly larger in the second baseline compared to the first. Therefore, we conclude that wall motion, coronary flow, and hemodynamics recovered adequately between the two stress tests.

One potential limitation of the analysis outlined here relates to defining 3DFS relative to the average response to DSE in normal hearts. Clinical application of 3DFS as defined here will require establishing the average response to 3DFS at peak stress in the absence of ischemia as a baseline for comparison. The size, shape, and function of the canine hearts in this study were fairly homogenous, so 3DFS in the CTRL peak stress images used for normalization had low variability. Patients who undergo DSE and prove to have no clinically significant coronary artery disease likely will display more 3DFS variability; if this variability proves limiting in defining a uniform threshold for detecting critical stenoses clinically, an alternate approach would be to focus on the regional changes in 3DFS between baseline and stress in individual patients, an approach we have taken in prior animal studies.¹⁵ A second limitation of this study is that it was powered to test the ability of individual mechanical measures to separate cases with $CFR < 1.1$ from those with $CFR > 1.1$ using ROC analysis, but not to test for statistical differences between mechanical measures in making that determination. From an ROC power analysis⁴⁵ we estimate that $n=80$ experiments would be necessary to statistically differentiate between the measures with largest and smallest AUC in this study, area strain and longitudinal strain. Our data therefore should not be used to draw definitive conclusions regarding the relative ability of various strain measures to detect critical stenoses. Finally, compared to the way these measures would be used in clinical practice, our comparison of 3DFS and strain likely placed strain at a disadvantage for predicting PD size and 3DFS at a disadvantage for detecting the presence of a critical stenosis. We measured 3DFS over the entire LV surface but strain only at one location in the LAD perfusion region. If strain were measured over the entire LV

using 3D speckle tracking, it might also provide useful information on the size, location, and severity of a wall motion abnormality during stress testing. On the other hand, we measured strain by sonomicrometry, which is the invasive gold standard for measuring strain, giving strains a potential advantage over 3DFS in identifying ischemic regions in this study. Despite these limitations, our data and Monte Carlo simulation suggest that the sensitivity and specificity of 3DFS is comparable to 2D circumferential strain or 3D area strain measured with current speckle tracking technology.

The scope of this study was limited to evaluating mechanical measures in the case of single vessel critical stenoses. The optimal thresholds for this criteria resulted in high specificity in detecting critical stenoses but lower sensitivity to mild ischemia, as illustrated in Figure 4B. These results are similar to the higher specificity and lower sensitivity of stress echocardiography with visual diagnosis of wall motion abnormalities compared with perfusion imaging,²⁶ and likely indicate a limitation of wall motion for sensitivity to CAD. An ideal clinical measure would also be sensitive to wall motion abnormalities caused by multi-vessel disease or microvascular disease. While these applications have yet to be tested, defining 3DFS relative to a standard normal response in patients without ischemia instead of focusing on regional differences in the stress response could have advantages in detecting multi vessel disease.

Finally, our methods were tested in the limited case of an LAD critical stenosis, which clinically is often a severe injury and easy to detect. However, the severity of mechanical dysfunction and perfusion defects caused by these stenoses varied significantly between animals, and on average induced only modest reductions in end systolic pressure and systolic shortening. This is likely due to the strong collateral perfusion in the canine model. The critical stenoses in this study, defined by LAD flow, are likely analogous to milder stenoses in a clinical setting.

CONCLUSION

The present study demonstrates that quantitative wall motion analysis using 3DFS can be used to detect a critical stenosis during DSE with sensitivity and specificity similar to 3D strain. In addition, 3DFS provides potentially useful new information on the size and location of a PD. This quantitative analysis method shows promise for improving and quantifying diagnosis of CAD from cardiac stress testing.

Acknowledgments

This work was supported by an AHA Predoctoral Fellowship (KMP) and NIH R01 HL 085160 (JWH).

References

1. Hoffmann R, Lethen H, Marwick T, et al. Analysis of interinstitutional observer agreement in interpretation of dobutamine stress echocardiograms. *J Am Coll Cardiol.* 1996; 27:330–6. [PubMed: 8557902]
2. Picano E, Lattanzi F, Orlandini A, et al. Stress echocardiography and the human factor: the importance of being expert. *J Am Coll Cardiol.* 1991; 17:666–9. [PubMed: 1993786]

3. Mor Avi V, Lang RM, Badano LP, et al. Current and Evolving Echocardiographic Techniques for the Quantitative Evaluation of Cardiac Mechanics: ASE/EAE Consensus Statement on Methodology and Indications Endorsed by the Japanese Society of Echocardiography. *J Am Soc Echocardiogr.* 2011; 24:277–313. [PubMed: 21338865]
4. Moynihan PF, Parisi AF, Feldman CL. Quantitative detection of regional left ventricular contraction abnormalities by two dimensional echocardiography. I. Analysis of methods. *Circulation.* 1981; 63:752–60. [PubMed: 7471329]
5. Mor Avi V, Vignon P, Koch R, et al. Segmental Analysis of Color Kinesis Images: New Method for Quantification of the Magnitude and Timing of Endocardial Motion During Left Ventricular Systole and Diastole. *Circulation.* 1997; 95:2082–97. [PubMed: 9133519]
6. Amundsen BH, Helle Valle T, Edvardsen T, et al. Noninvasive myocardial strain measurement by speckle tracking echocardiography: validation against sonomicrometry and tagged magnetic resonance imaging. *J Am Coll Cardiol.* 2006; 47:789–93. [PubMed: 16487846]
7. Reant P, Labrousse L, Lafitte S, et al. Experimental validation of circumferential, longitudinal, and radial 2 dimensional strain during dobutamine stress echocardiography in ischemic conditions. *J Am Coll Cardiol.* 2008; 51:149–57. [PubMed: 18191740]
8. Urheim S, Edvardsen T, Torp H, et al. Myocardial strain by Doppler echocardiography. Validation of a new method to quantify regional myocardial function. *Circulation.* 2000; 102:1158–64. [PubMed: 10973846]
9. Voigt JU, Exner B, Schmiedehausen K, et al. Strain rate imaging during dobutamine stress echocardiography provides objective evidence of inducible ischemia. *Circulation.* 2003; 107:2120–6. [PubMed: 12682001]
10. Marwick TH. Measurement of strain and strain rate by echocardiography: ready for prime time? *J Am Coll Cardiol.* 2006; 47:1313–27. [PubMed: 16580516]
11. Wiske PS, Pearlman JD, Hogan RD, et al. Echocardiographic definition of the left ventricular centroid. II. Determination of the optimal centroid during systole in normal and infarcted hearts. *J Am Coll Cardiol.* 1990; 16:993–9. [PubMed: 2212382]
12. Bansal M, Cho GY, Chan J, et al. Feasibility and accuracy of different techniques of two-dimensional speckle based strain and validation with harmonic phase magnetic resonance imaging. *J Am Soc Echocardiogr.* 2008; 21:1318–25. [PubMed: 19041575]
13. Aggeli C, Giannopoulos G, Misovoulos P, et al. Real time three dimensional dobutamine stress echocardiography for coronary artery disease diagnosis: validation with coronary angiography. *Heart.* 2007; 93:672–5. [PubMed: 17085530]
14. Herz SL, Ingrassia CM, Homma S, et al. Parameterization of Left Ventricular Wall Motion for Detection of Regional Ischemia. *Ann Biomed Eng.* 2005; 33:912–19. [PubMed: 16060531]
15. Herz SL, Hasegawa T, Makaryus AN, et al. Quantitative three dimensional wall motion analysis predicts ischemic region size and location. *Ann Biomed Eng.* 2010; 38:1367–76. [PubMed: 20069372]
16. Seo Y, Ishizu T, Enomoto Y, et al. Validation of 3 dimensional speckle tracking imaging to quantify regional myocardial deformation. *Circ Cardiovasc Imaging.* 2009; 2:451–9. [PubMed: 19920043]
17. Seo Y, Ishizu T, Enomoto Y, et al. Endocardial surface area tracking for assessment of regional LV wall deformation with 3D speckle tracking imaging. *JACC Cardiovasc Imaging.* 2011; 4:358–65. [PubMed: 21492810]
18. Kleijn, S a; Aly, MF a; Terwee, CB., et al. Three dimensional speckle tracking echocardiography for automatic assessment of global and regional left ventricular function based on area strain. *J Am Soc Echocardiogr.* 2011; 24:314–21. [PubMed: 21338866]
19. Calnon DA, Glover DK, Beller GA, et al. Effects of dobutamine stress on myocardial blood flow, ^{99m}Tc sestamibi uptake, and systolic wall thickening in the presence of coronary artery stenoses: implications for dobutamine stress testing. *Circulation.* 1997; 96:2353–60. [PubMed: 9337211]
20. Holmes JW. Candidate mechanical stimuli for hypertrophy during volume overload. *J Appl Physiol.* 2004; 97:1453–60. [PubMed: 15169750]
21. Fomovsky GM, Clark SA, Parker KM, et al. Anisotropic reinforcement of acute anteroapical infarcts improves pump function. *Circ Hear. Fail.* 2012; 5:515–22.

22. Ingul CB, Torp H, Aase SA, et al. Automated analysis of strain rate and strain: feasibility and clinical implications. *J Am Soc Echocardiogr.* 2005; 18:411–8.
23. Bjork Ingul C, Rozis E, Slordahl SA, et al. Incremental value of strain rate imaging to wall motion analysis for prediction of outcome in patients undergoing dobutamine stress echocardiography. *Circulation.* 2007; 115:1252–9. [PubMed: 17325245]
24. Amundsen BH, Crosby J, Steen PA, et al. Regional myocardial long axis strain and strain rate measured by different tissue Doppler and speckle tracking echocardiography methods: a comparison with tagged magnetic resonance imaging. *Eur J Echocardiogr.* 2009; 10:229–37. [PubMed: 18650220]
25. Bland JM, Altman DG. Statistical methods for assessing agreement between two methods of clinical measurement. *Lancet.* 1986; i:307–310. [PubMed: 2868172]
26. Pellikka PA, Nagueh SF, Elhendy AA, et al. American Society of Echocardiography recommendations for performance, interpretation, and application of stress echocardiography. *J Am Soc Echocardiogr.* 2007; 20:1021–41. [PubMed: 17765820]
27. Leong Poi H, Rim SE, Le DE, et al. Perfusion versus function: the ischemic cascade in demand ischemia: implications of single vessel versus multivessel stenosis. *Circulation.* 2002; 105:987–92. [PubMed: 11864930]
28. Lima JA, Becker LC, Melin JA, et al. Impaired thickening of nonischemic myocardium during acute regional ischemia in the dog. *Circulation.* 1985; 71:1048–59. [PubMed: 3986975]
29. Kerber R, Marcus M, Ehrhardt J, et al. Correlation between echocardiographically demonstrated segmental dyskinesia and regional myocardial perfusion. *Circulation.* 1975; 52:1097–104. [PubMed: 1182955]
30. Tanaka H, Oishi Y, Mizuguchi Y, et al. Three dimensional evaluation of dobutamine induced changes in regional myocardial deformation in ischemic myocardium using ultrasonic strain measurements: the role of circumferential myocardial shortening. *J Am Soc Echocardiogr.* 2007; 20:1294–99. [PubMed: 17604959]
31. Reant P, Labrousse L, Lafitte S, et al. Quantitative analysis of function and perfusion during dobutamine stress in the detection of coronary stenoses: two dimensional strain and contrast echocardiography investigations. *J Am Soc Echocardiogr.* 2010; 23:95–103. [PubMed: 19962857]
32. Korosoglou G, Lehrke S, Wochele A, et al. Strain encoded CMR for the detection of inducible ischemia during intermediate stress. *JACC Cardiovasc Imaging.* 2010; 3:361–71. [PubMed: 20394897]
33. Villarreal FJ, Lew W, Waldman LK, et al. Transmural myocardial deformation in the ischemic canine left ventricle. *Circ Res.* 1991; 68:368–81. [PubMed: 1991344]
34. Uematsu M, Miyatake K, Tanaka N, et al. Myocardial velocity gradient as a new indicator of regional left ventricular contraction: detection by a two dimensional tissue Doppler imaging technique. *J Am Coll Cardiol.* 1995; 26:217–23. [PubMed: 7797755]
35. Yip G, Khandheria B, Belohlavek M, et al. Strain echocardiography tracks dobutamine-induced decrease in regional myocardial perfusion in nonocclusive coronary stenosis. *J Am Coll Cardiol.* 2004; 44:1664–71. [PubMed: 15489101]
36. Vatner SF. Correlation between acute reductions in myocardial blood flow and function in conscious dogs. *Circ Res.* 1980; 47:201–7. [PubMed: 7397952]
37. Gallagher K, Matsuzaki M, Koziol J, et al. Regional myocardial perfusion and wall thickening during ischemia in conscious dogs. *Am J Physiol.* 1984; 247:H727–38. [PubMed: 6496754]
38. Leong Poi H, Coggins MP, Sklenar J, et al. Role of collateral blood flow in the apparent disparity between the extent of abnormal wall thickening and perfusion defect size during acute myocardial infarction and demand ischemia. *J Am Coll Cardiol.* 2005; 45:565–72. [PubMed: 15708705]
39. Nemes A, Geleijnse ML, Krenning BJ, et al. Usefulness of ultrasound contrast agent to improve image quality during real time three dimensional stress echocardiography. *Am J Cardiol.* 2007; 99:275–8. [PubMed: 17223433]
40. Mor Avi V, Jenkins C, Kühl HP, et al. Real time 3 dimensional echocardiographic quantification of left ventricular volumes: multicenter study for validation with magnetic resonance imaging and investigation of sources of error. *JACC Cardiovasc Imaging.* 2008; 1:413–23. [PubMed: 19356461]

41. Parker KM. Regional Mechanics of Demand Ischemia During Cardiac Stress Testing. 2013:1–196.
42. Chang SA, Lee SC, Kim EY, et al. Feasibility of Single Beat Full Volume Capture Real Time Three Dimensional Echocardiography and Auto Contouring Algorithm for Quantification of Left Ventricular Volume: Validation with Cardiac Magnetic Resonance Imaging. *J Am Soc Echocardiogr.* 2011:C.
43. Leung KYE, Danilouchkine MG, van Stralen M, et al. Left ventricular border tracking using cardiac motion models and optical flow. *Ultrasound Med Biol.* 2011; 37:605–16. [PubMed: 21376448]
44. Yodwut C, Weinert L, Klas B, et al. Effects of frame rate on three dimensional speckle-tracking based measurements of myocardial deformation. *J Am Soc Echocardiogr.* 2012; 25:978–85. [PubMed: 22766029]
45. Obuchowski NA, Lieber ML, Wians FH. ROC curves in clinical chemistry: uses, misuses, and possible solutions. *Clin Chem.* 2004; 50:1118–25. [PubMed: 15142978]

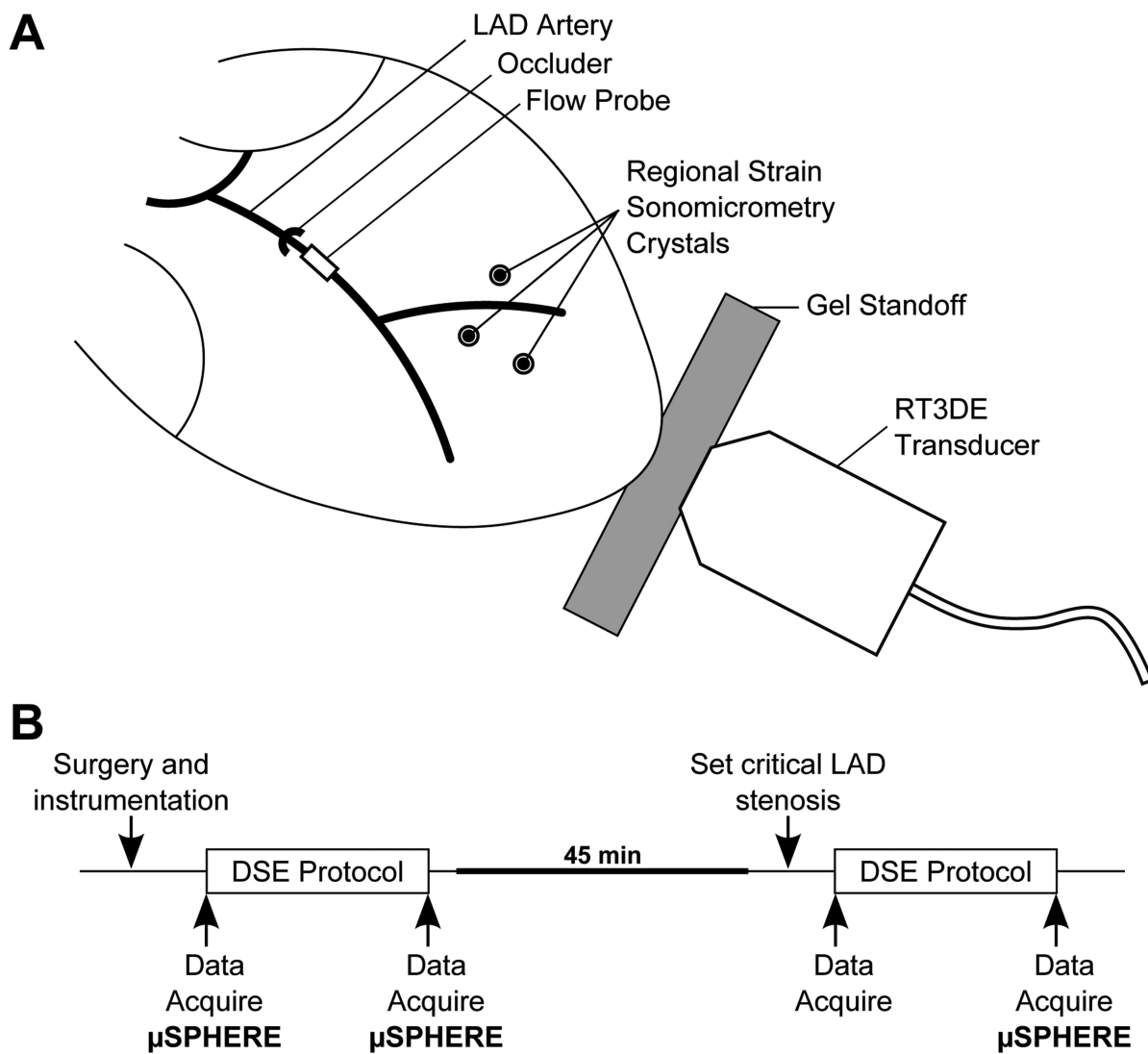


Figure 1. Experimental methods. **(A)** Experimental setup of the canine open-chest experiment. **(B)** Experimental protocol. Dobutamine stress echocardiography (DSE) is repeated with (STEN) and without (CTRL) a critical LAD stenosis. Data, including left ventricular pressure, regional strain, global function, LAD flow, and 3DE images, are collected as indicated. μ SPHERE indicates microsphere injection for quantification of regional blood flow.

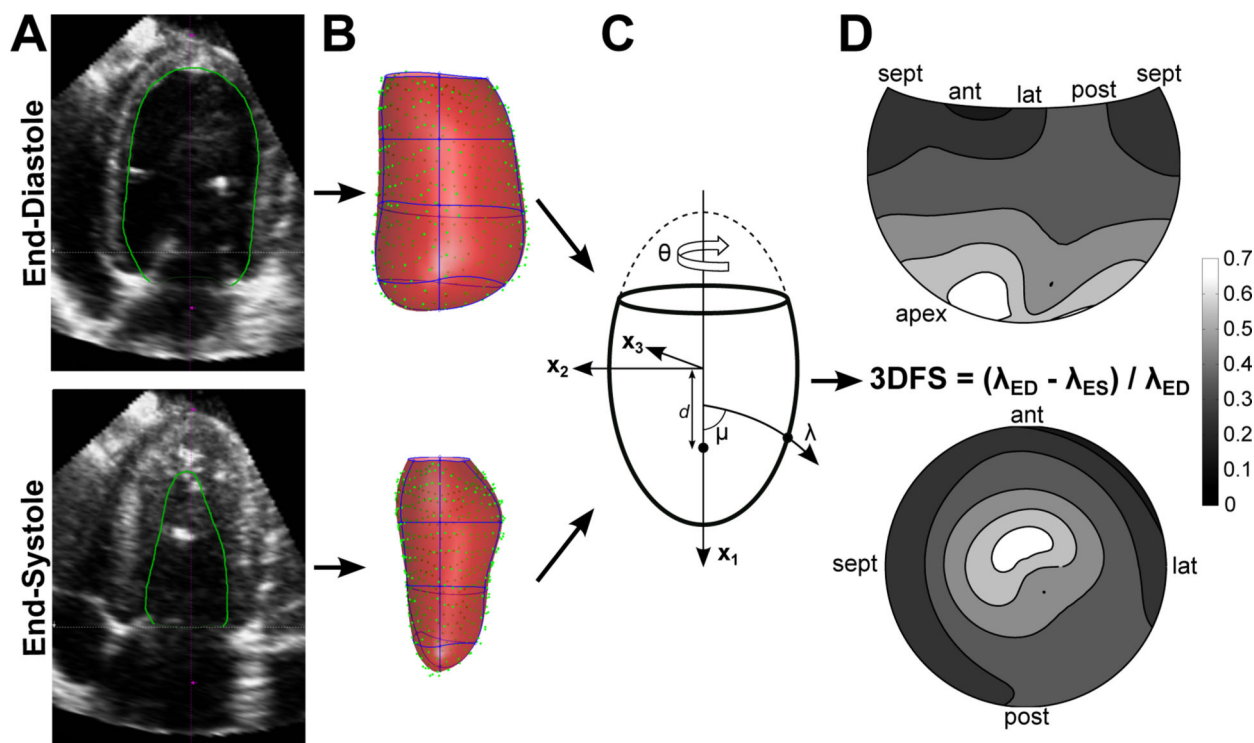


Figure 2.

Wall motion analysis methods demonstrated during CTRL peak stress. **(A)** Apical 4 chamber view of the 3DE image. The endocardial border was segmented (green) at end-diastole and end-systole using Tomtec 4D-LV Analysis software. **(B)** Data points representing the segmented surface (green) were exported and fit with a parametric surface (red, element borders blue, data and surfaces rotated 180° relative to images in (A)). **(C)** Surfaces were fit in prolate spheroidal coordinates, diagrammed here. Cartesian coordinates (x_1 , x_2 , x_3) are transformed into curvilinear coordinates (λ , μ , θ), scaled by the focal length d . **(D)** Average three-dimensional fractional shortening (3DFS) at peak stress during CTRL experiments is displayed on a Hammer projection map (top) and a standard bulls-eye map (bottom) representing the LV surface.

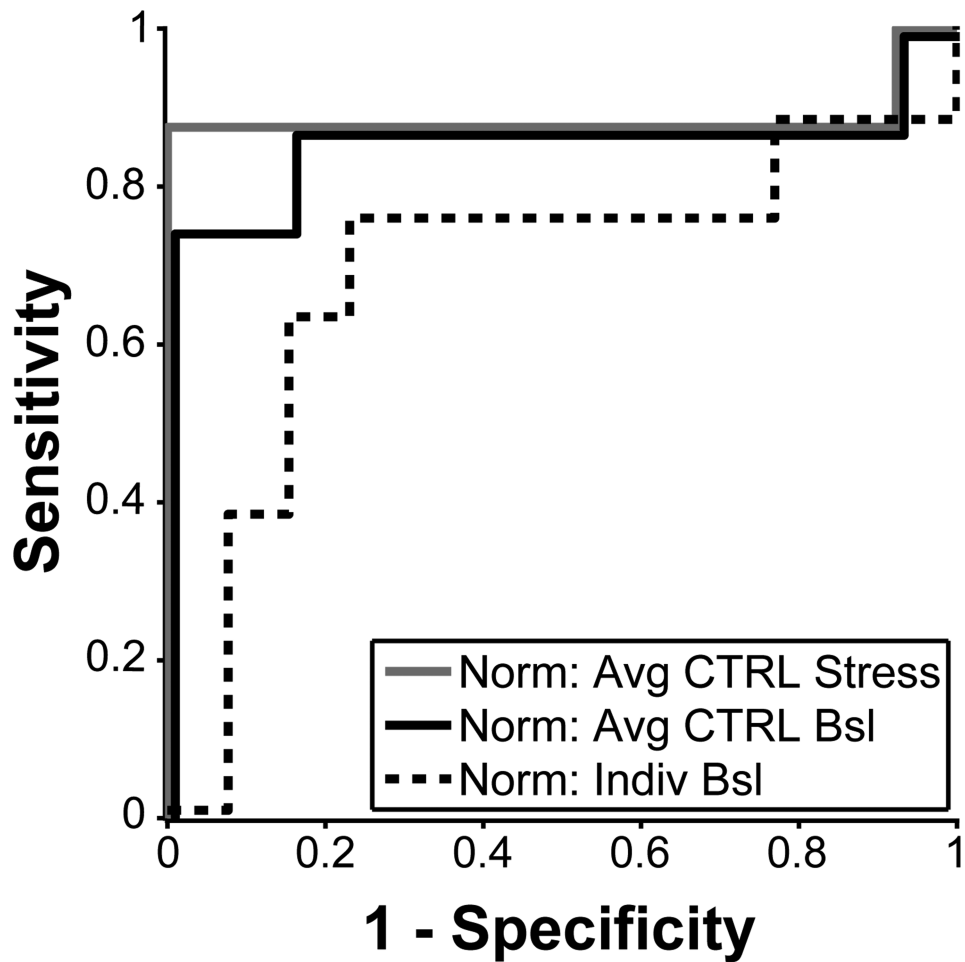


Figure 3.

By ROC analysis, normalizing 3DFS by average 3DFS during CTRL peak stress is more sensitive and specific for separating $CFR < 1.1$ from $CFR > 1.1$ than normalizing by average 3DFS during CTRL baseline or by baseline 3DFS of each individual case.

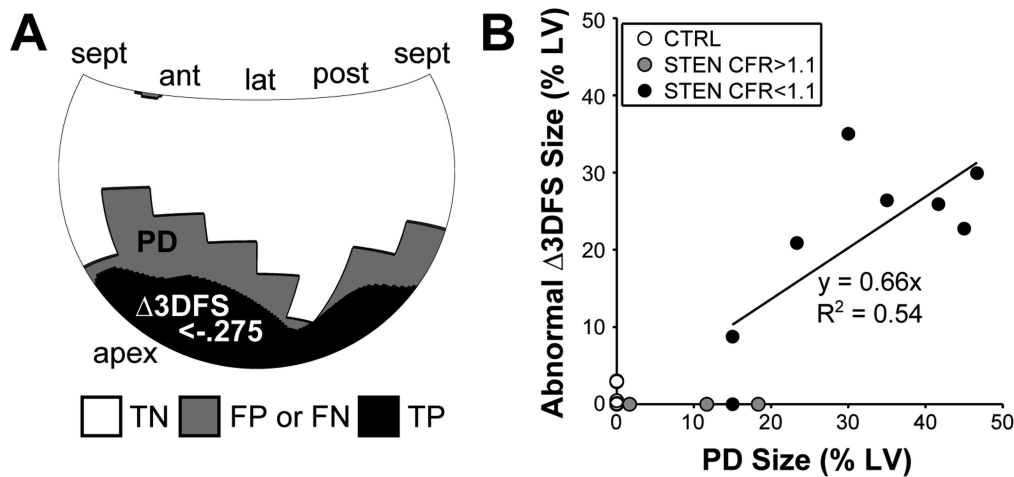


Figure 4. By calculating the area of the LV surface with $\Delta 3DFS$ below an optimum threshold, we can measure the size and location of a wall motion abnormality. **(A)** In a typical example, the area with $\Delta 3DFS$ below the optimal threshold is contained within the PD region determined by microspheres. Regions are classified by a true positive (TP) or true negative (TN) match between the PD region and abnormal $\Delta 3DFS$ region, or false positive (FP) or false negative (FN) mismatch. **(B)** Across all experiments where $CFR < 1.1$, the size of the $\Delta 3DFS$ abnormality correlates well with PD region size.

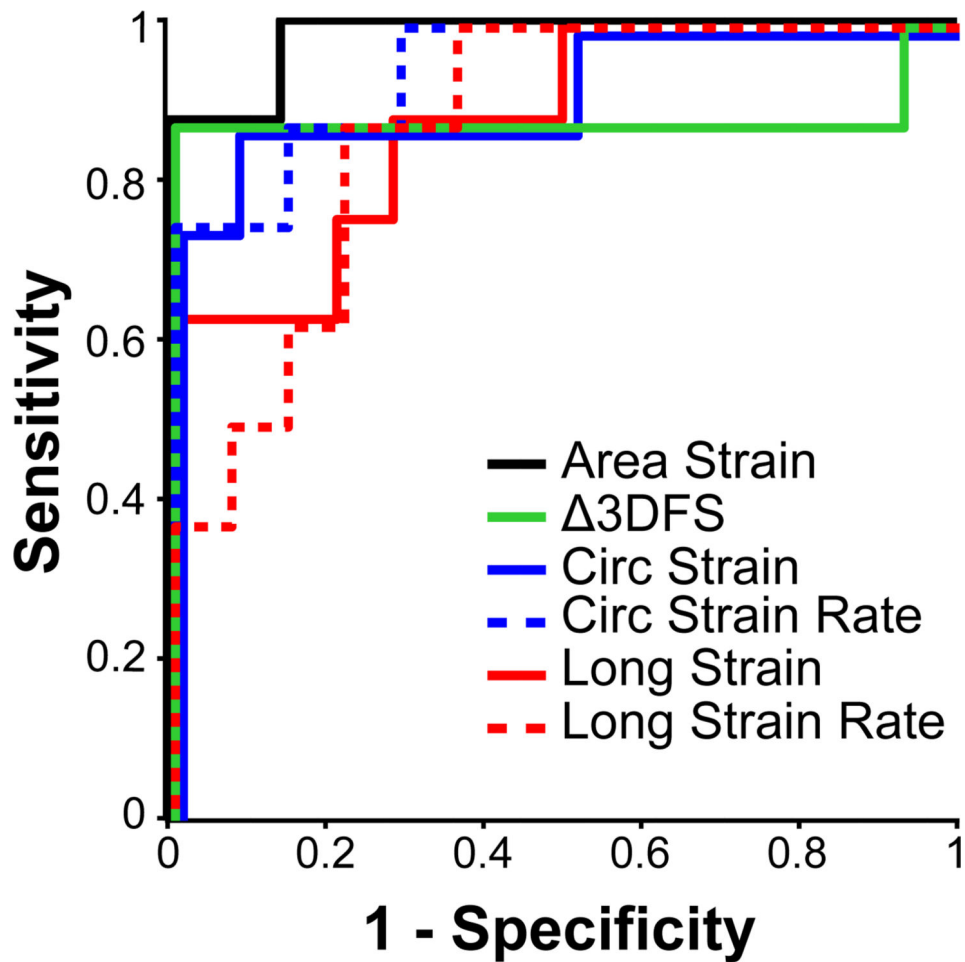


Figure 5. Receiver operating characteristic (ROC) analysis shows the utility of each measure for separating CFR<1.1 from CFR>1.1 and CTRL. All curves overlap at sensitivity <0.3 and =1.0 but are offset slightly for better visibility.

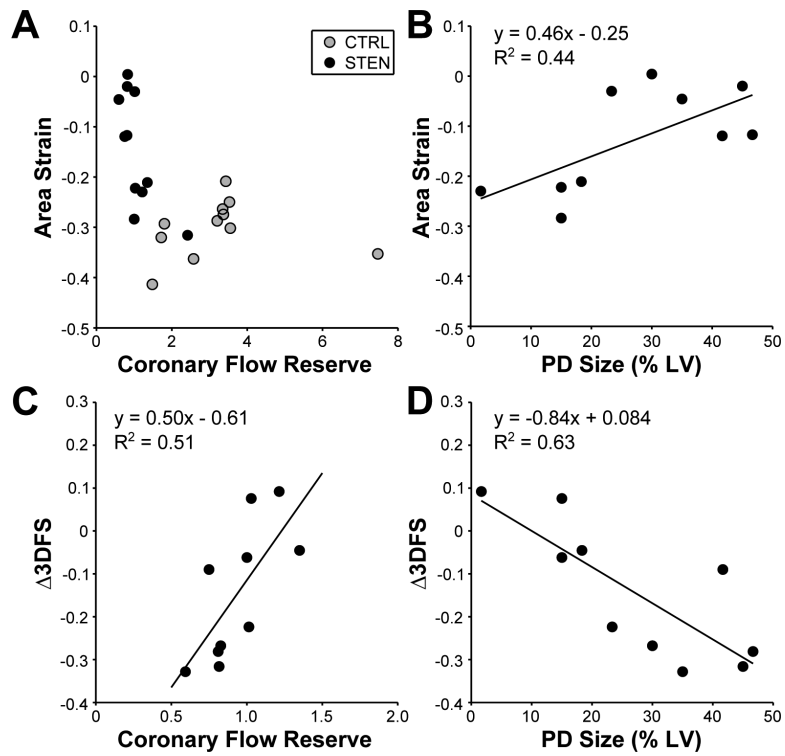


Figure 6. Area strain displays the expected exponential flow-function relationship with CFR in both CTRL and STEN (A). When focusing on cases in which $CFR < 2.0$, a significant relationship was found between area strain and PD size (B) and $\Delta 3DFS$ and CFR (C) and PD size (D).

Table 1

Hemodynamic parameters

| | Baseline | CTRL Stress | STEN Stress |
|-------------------|-------------|--------------|--------------|
| HR (bpm) | 97 ± 13 | 171 ± 23 | 177 ± 29 |
| EDV (mL) | 36.7 ± 8.5 | 36.4 ± 10.6 | 39.1 ± 6.5 |
| ESV (mL) | 17.5 ± 5.3 | 11.0 ± 2.8 | 14.3 ± 6.8 |
| EF (%) | 52.5 ± 6.8 | 69.2 ± 6.0 | 63.8 ± 15.0 |
| CO (L/min) | 1.85 ± 0.46 | 4.19 ± 0.91 | 4.24 ± 0.70 |
| EDP (mmHg) | 8.1 ± 3.1 | 8.4 ± 2.9 | 9.1 ± 2.3 |
| ESP (mmHg) | 77.9 ± 8.5 | 104.8 ± 13.6 | 94.4 ± 20.2* |
| LAD flow (mL/min) | 40.5 ± 23.1 | 108.9 ± 36.3 | 20.4 ± 7.6* |

Values are mean ± SD (n=10 for CTRL peak stress, n=11 otherwise). HR = heart rate; EDV = end-diastolic volume; ESV = end-systolic volume; EF = ejection fraction; CO = cardiac output; EDP = end-diastolic pressure; ESP = end-systolic pressure; LAD = left anterior descending artery

* Indicates significantly different from CTRL by paired t-test.

Table 2

ROC characteristics of measures of regional mechanics.

| | Sensitivity | Specificity | AUC |
|--------------|--------------------|--------------------|------------|
| 3DFS | 88% | 100% | 0.885 |
| Area Strain | 88% | 100% | 0.982 |
| Circ Strain | 88% | 92% | 0.929 |
| Long Strain | 88% | 71% | 0.875 |
| Peak SR Circ | 88% | 86% | 0.946 |
| Peak SR Long | 88% | 79% | 0.875 |

3DFS = Three-dimensional fractional shortening, SR = strain rate, ROC = receiver operating characteristic, AUC = area under the ROC curve.

Author Manuscript

Author Manuscript

Author Manuscript

Author Manuscript

Table 3

Multiple linear regression parameters and significance

| <i>Y</i> | CFR | | | PD size | | |
|---------------------|-----------------------|--------------|----------------|-----------------------|--------------|----------------|
| | <i>R</i> ² | <i>Slope</i> | <i>p-value</i> | <i>R</i> ² | <i>Slope</i> | <i>p-value</i> |
| 3DFS | 0.71 | 0.50 | 0.021 | 0.79 | -0.84 | 0.006 |
| Area strain | 0.63 | -0.29 | 0.052 | 0.67 | 0.46 | 0.035 |
| Circ strain | 0.50 | -0.17 | 0.139 | 0.53 | 0.28 | 0.113 |
| Long strain | 0.41 | -0.07 | 0.243 | 0.20 | 0.05 | 0.585 |
| Peak SR Circ | 0.50 | -1.68 | 0.144 | 0.40 | 2.03 | 0.257 |
| Peak SR Long | 0.12 | 0.32 | 0.733 | 0.09 | -0.33 | 0.814 |

3DFS = three-dimensional fractional shortening, CFR = coronary flow reserve, PD = perfusion defect.

Author Manuscript

Author Manuscript

Author Manuscript

Author Manuscript

Table 4

Monte Carlo simulation of speckle tracking strain performance

| | Modality | Predicted AUC | Sensitivity (%) | Specificity (%) |
|--------------------|----------|---------------|-----------------|-----------------|
| Area Strain | 3D | 0.90 ± 0.06 | 87 ± 9 | 87 ± 10 |
| Circ Strain | 3D | 0.85 ± 0.07 | 85 ± 10 | 83 ± 9 |
| Long Strain | 3D | 0.75 ± 0.09 | 75 ± 12 | 76 ± 12 |
| Circ Strain | 2D | 0.92 ± 0.03 | 93 ± 7 | 88 ± 4 |
| Long Strain | 2D | 0.83 ± 0.05 | 81 ± 10 | 79 ± 10 |

Author Manuscript

Author Manuscript

Author Manuscript

Author Manuscript